We are IntechOpen, the world's leading publisher of Open Access books Built by scientists, for scientists

6,900
Open access books available

185,000
International authors and editors

200M
Downloads

Our authors are among the

154
Countries delivered to

TOP 1%
most cited scientists

12.2%
Contributors from top 500 universities



WEB OF SCIENCE™

Selection of our books indexed in the Book Citation Index in Web of Science™ Core Collection (BKCI)

Interested in publishing with us?
Contact book.department@intechopen.com

Numbers displayed above are based on latest data collected.
For more information visit www.intechopen.com



Chapter 14

Reconfigurable Microstrip Antennas for Cognitive Radio

Mohammed Al-Husseini, Karim Y. Kabalan,
Ali El-Hajj and Christos G. Christodoulou

Additional information is available at the end of the chapter

http://dx.doi.org/10.5772/53430

1. Introduction

An increasing demand for radio spectrum has resulted from the emergence of feature-rich and high-data-rate wireless applications. The spectrum is scarce, and the current radio spectrum regulations make its use inefficient. This necessitates the development of new dynamic spectrum allocation policies to better exploit the existing spectrum.

According to the current spectrum allocation regulations, specific bands are assigned to particular services, and only licensed users are granted access to licensed bands. Cognitive radio (CR) is expected to revolutionize the way spectrum is allocated. In a CR network, the intelligent radio part allows unlicensed users (secondary users) to access spectrum bands licensed to primary users, while avoiding interference with them.

Two approaches to sharing spectrum between primary and secondary users have been considered: spectrum underlay and spectrum overlay. In the underlay approach, secondary users should operate below the noise floor of primary users, and thus severe constraints are imposed on their transmission power. Ultra-wideband (UWB) technology is very suitable as the enabling technology for this approach. In spectrum overlay CR, secondary users search for unused frequency bands, called white spaces, and use them for communication.

In this chapter, we report and discuss antenna designs for overlay and underlay CR. We start by studying techniques employed in the design of UWB antennas. This is done in Section 3. Such antennas are used for underlay CR, but also for channel sensing in overlay CR. We then move in Section 4 to antennas that allow the use of UWB in overlay CR. These are basically UWB antennas, but have the ability to selectively induce frequency notches in the bands of primary services, thus preventing any interference to them and giving the UWB transmitters used by the secondary users the chance to increase their power, and hence to achieve long-distance communication. In Section 5, we investigate the design of antennas for overlay CR. In this scheme, an antenna should be able to monitor the spectrum (sensing),

INTECH
open science | open minds

© 2013 Al-Husseini et al.; licensee InTech. This is an open access article distributed under the terms of the Creative Commons Attribution License (http://creativecommons.org/licenses/by/3.0), which permits unrestricted use, distribution, and reproduction in any medium, provided the original work is properly cited.

and communicate over a chosen white space (communication). For the latter operation, the antenna must be frequency-reconfigurable. Single- and dual-port antennas for overlay CR can be designed. In the dual-port case, one port has UWB frequency response and is used for channel sensing, and the second port, which is frequency-reconfigurable, is used for communicating. In the more challenging single-port design, the same port can have UWB response for sensing, and can be reconfigured for tunable narrowband operation when required to communicate over a white space.

2. Dynamic spectrum access and cognitive radio

The increasing demand for wireless connectivity and current crowding of licensed and unlicensed spectra necessitate a new communication paradigm to exploit the existing spectrum in better ways. The current approach for spectrum allocation is based on assigning a specific band to a particular service. The FCC Spectrum Policy Task Force [1] reported vast temporal and geographic variations in the usage of allocated spectrum with utilization ranging from 15 to 85% in the bands below 3 GHz. In the frequency range above 3 GHz the bands are even more poorly utilized. In other words, a large portion of the assigned spectrum is used sporadically, leading to an under utilization of a significant amount of spectrum. This inefficiency arises from the inflexibility of the regulatory and licensing process, which typically assigns the complete rights to a frequency band to a primary user. This approach makes it extremely difficult to recycle these bands once they are allocated, even if these users poorly utilize this valuable resource. A solution to this inefficiency, which has been highly successful in the ISM (2.4 GHz), the U-NII (5–6 GHz), and microwave (57–64 GHz) bands, is to make spectra available on an unlicensed basis. However, in order to obtain spectra for unlicensed operation, new sharing concepts have been introduced to allow use by secondary users under the requirement that they limit their interference to pre-existing primary users.

2.1. Cognitive radio

Cognitive radio (CR) technology is key enabling technology which provides the capability to share the wireless channel with the licensed users in an opportunistic way. CRs are foreseen to be able to provide the high bandwidth to mobile users via heterogeneous wireless architectures and dynamic spectrum access techniques.

In order to share the spectrum with licensed users without interfering with them, and meet the diverse quality of service requirements of applications, each CR user in a CR network must [2]:

- Determine the portion of spectrum that is available, which is known as Spectrum sensing.
- Select the best available channel, which is called Spectrum decision.
- Coordinate access to this channel with other users, which is known as Spectrum sharing.
- Vacate the channel when a licensed user is detected, which is referred as Spectrum mobility.

To fulfill these functions of spectrum sensing, spectrum decision, spectrum sharing and spectrum mobility, a CR has to be cognitive, reconfigurable and self-organized. An example of the cognitive capability is the CR's ability to sense the spectrum and detect spectrum holes (also called white spaces), which are those frequency bands not used by the licensed users. The reconfigurable capability can be summarized by the ability to dynamically

choose the suitable operating frequency (frequency agility), and the ability to adapt the modulation/coding schemes and transmit power as needed. The self-organized capability has to do with the possession of a good spectrum management scheme, a good mobility and connection management, and the ability to to support security functions in dynamic environments.

2.2. Spectrum sharing approaches

Dynamic spectrum access (DSA) represents the opposite direction of the current static spectrum management policy. It is broadly categorized under three models: the dynamic exclusive use model, the open sharing model, and the hierarchical access model. The taxonomy of DSA is illustrated in Fig. 1 [3].

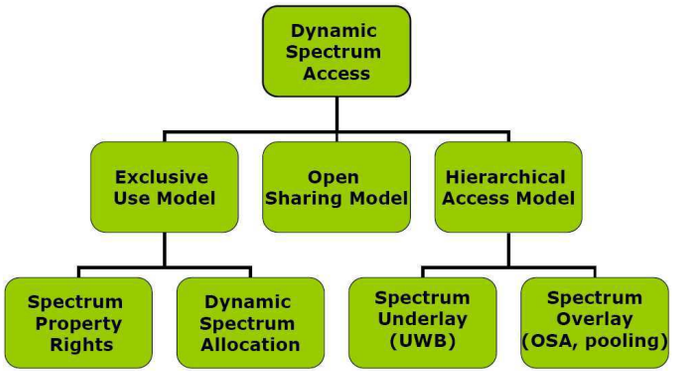


Figure 1. Dynamic spectrum access models [3]

In the dynamic exclusive use model, the spectrum bands are still licensed to services for exclusive use, as in the current spectrum regulation policy, but flexibility is introduced to improve spectrum efficiency. Two approaches have been proposed under this model: spectrum property rights and dynamic spectrum allocation. The first approach, the spectrum property rights, allows licensees to sell and trade spectrum and to freely choose technology. In the second approach, the dynamic spectrum allocation, the aim is to improve spectrum efficiency through dynamic spectrum assignment by exploiting the spatial and temporal traffic statistics of different services.

The open sharing model employs open sharing among peer users as the basis for managing a spectral region. Supporters of this model rely on the huge success of wireless services operating in the ISM band.

A hierarchical access structure with primary and secondary users is adopted by the third model. Here, the spectrum licensed to primary users is open to secondary users while limiting interference to the primary users. Two approaches to spectrum sharing between primary and secondary users have been considered: spectrum underlay and spectrum overlay.

In the underlay approach, secondary users should operate below the noise floor of primary users, and thus severe constraints are imposed on their transmission power. One way to achieve this is to spread the transmitted signals of secondary users over an ultra-wide frequency band (UWB), leading to a short-range high data rate with extremely low

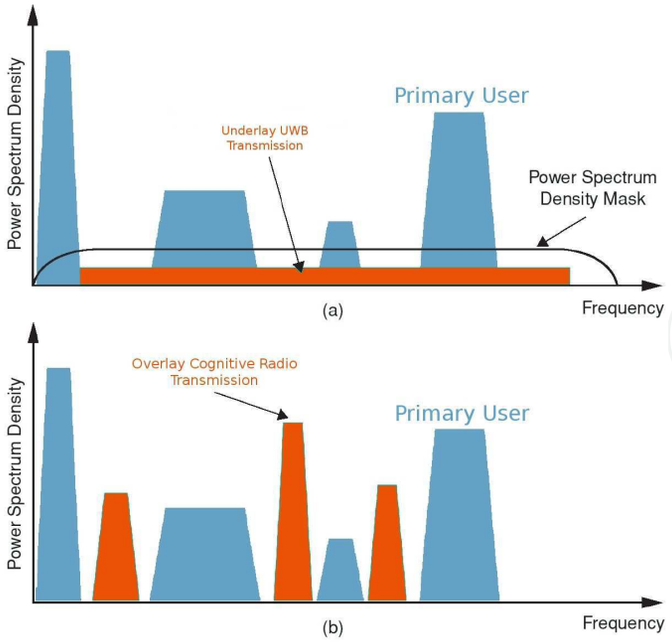


Figure 2. Underlay (a) and overlay (b) spectrum sharing approaches

transmission power (less than -42 dBm/MHz in the 3.1–10.6 GHz band). Assuming that primary users transmit all the time (worst case scenario), this approach does not rely on detection and exploitation of spectrum white space.

The spectrum overlay approach, also termed opportunistic spectrum access or OSA, imposes restrictions on when and where secondary users may transmit rather on their transmission power. In this approach, secondary users avoid higher priority users through the use of spectrum sensing and adaptive allocation. They identify and exploit the spectrum holes defined in space, time, and frequency.

The underlay and overlay approaches in the hierarchical model are illustrated in Fig. 2. They can be employed simultaneously for further spectrum efficiency improvement. Furthermore, the hierarchical model is more compatible with current spectrum management policies and legacy wireless systems as compared to the other two models.

3. UWB antennas

UWB antennas are required for underlay CR, and for sensing in overlay CR. UWB antennas were originally meant to radiate very short pulses over short distances. They have been used in medical applications, GPRs, and other short-range communications requiring high throughputs. The literature is rich with articles pertaining to the design of UWB antennas [4–9]. For example, the authors in [4] present a UWB knight's helm shape antenna fabricated on an FR4 board with a double slotted rectangular patch tapered from a 50-Ω feed line, and a partial ground plane flushed with the feed line. Three techniques are applied for good impedance matching over the UWB range: 1) the dual slots on the rectangular patch, 2) the tapered connection between the rectangular patch and the feed line, and 3) a partial ground plane flushed with the feed line. Consistent omnidirectional radiation patterns and a small group delay characterize this UWB antenna.

http://dx.doi.org/10.5772/53430

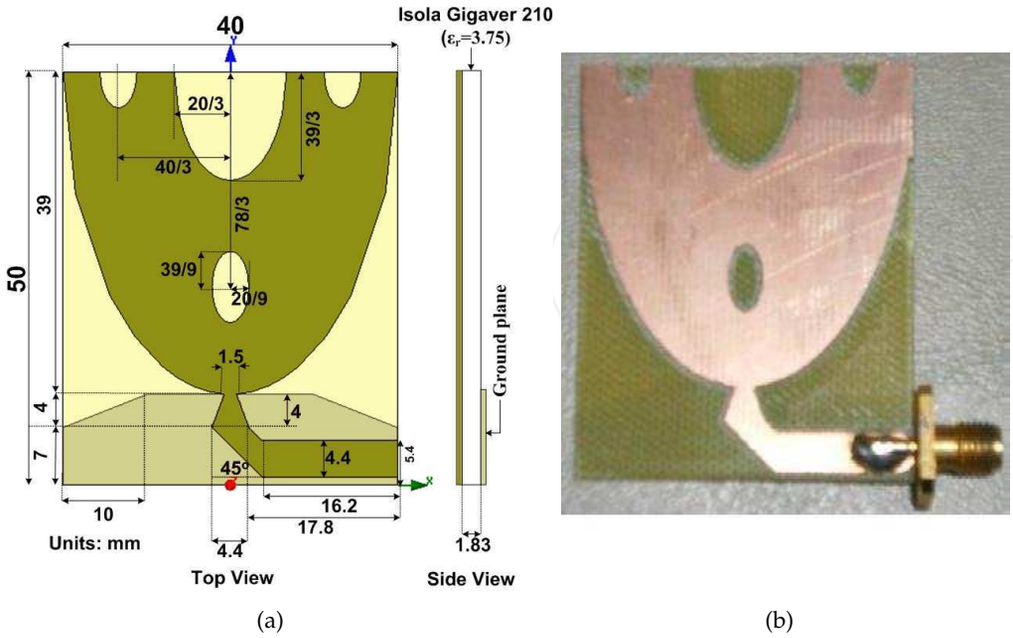
In general, the guidelines to design UWB antennas include:

- The proper selection of the patch shape. Round shapes and round edges lead to smoother current flow, and as a result to better wideband characteristics,
- The good design of the ground plane. Partial ground planes, and ground planes with specially designed slots, play a major role in obtaining UWB response. This property is discussed in 3.2,
- The matching between the feed line and the patch. This is achieved using either tapered connections, inset feed, or slits under the feed in the ground plane,
- The use of fractal shapes, which are known for their self-repetitive characteristic, used to obtain multi- and wide-band operation, and their space-filling property, which leads to increasing the electrical length of the antenna without tampering with its overall physical size.

To investigate the above guidelines, several UWB antennas have been designed [10–14]. Only two of them will be described in this Section.

3.1. Combination of UWB techniques

The UWB design presented in [12] features a microstrip feed line with two 45° bends and a tapered section for size reduction and matching, respectively. The ground plane is partial and comprises a rectangular part and a trapezoidal part. The patch is a half ellipse with the cut made along the minor axis. Four slots whose location and size relate to a modified Sierpinski carpet, with the ellipse as the basic shape, are incorporated into the patch. The configuration of this antenna is shown in Fig. 3.



(a) (b)

Figure 3. (a) Configuration and (b) photo of the UWB antenna in [12]. The antenna combines several bandwidth enhancement techniques.

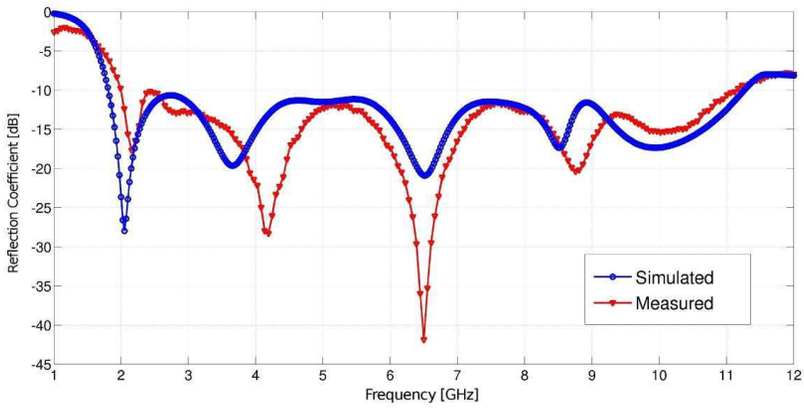


Figure 4. Reflection coefficient of the UWB antenna in Fig. 3

Four techniques are applied for good impedance matching over the UWB range: 1) the specially selected patch shape, 2) the tapered connection between the patch and the feed line, 3) the optimized partial ground plane, and 4) the slots whose design is based on the knowledge of fractal shapes. As a result, this antenna has an impedance bandwidth over the 2–11 GHz range, as shown in Fig. 4, and thus can operate in the bands used for UMTS, WLAN, WiMAX, and UWB applications. Consistent omnidirectional radiation patterns, and good gain and efficiency values characterize this UWB antenna. The radiation patterns are shown in Fig. 5.

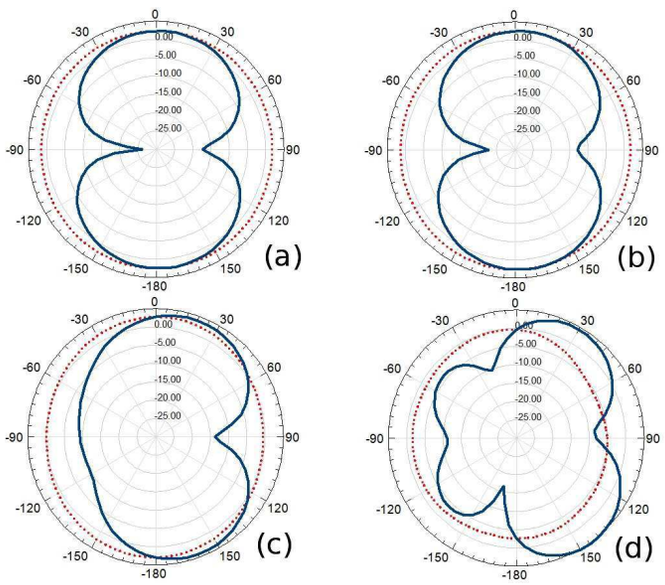


Figure 5. Patterns of the antenna in Fig. 3 in the X−Z plane (dotted line) and Y−Z plane (solid line) for (a) 2.1 GHz, (b) 2.4 GHz, (c) 3.5 GHz, and (d) 5.1 GHz

3.2. Effect of ground plane

The effect of the ground plane on the performance of UWB antennas is studied in [14–16]. The design in [14] is a coplanar-waveguide-fed antenna based on an egg-shaped conductor, and is taken as an example. The shape of the patch is suitable for UWB response. A large egg-shaped slot, with parametrized dimensions, was made in the ground, as shown in Fig. 6.

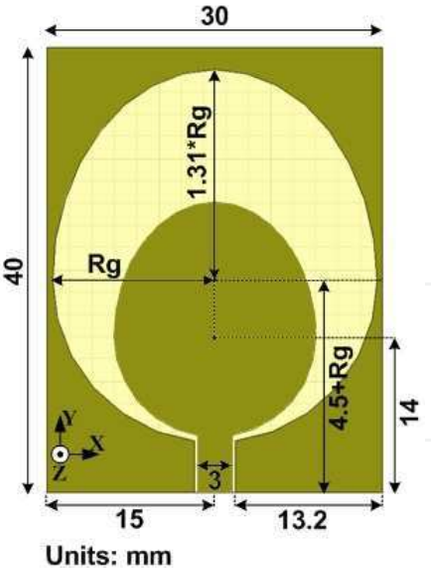
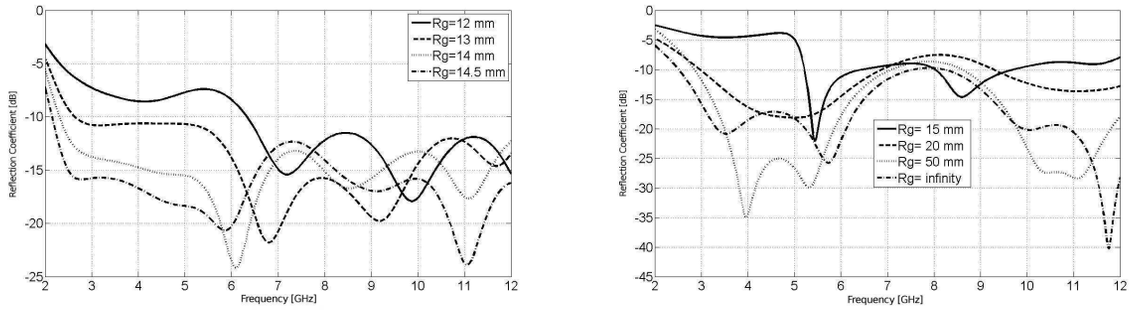


Figure 6. Design with parametrized ground plane slot [14]

The effect of changing the parameter R_g on the reflection coefficient is shown in Fig. 7. The results show that a slot of a specific size ($R_g = 14.5$ mm) results in a UWB response, so does a partial rectangular ground plane (corresponds to $R_g = \infty$). The configurations of these two optimal designs are shown in Fig. 8.



(a) (b)

Figure 7. Reflection coefficient of the antenna in Fig. 6 for different R_g values

The measured and computed reflection coefficients of the two optimal designs are given in Fig. 9. Since the studied antenna is the type of a printed monopole, both optimal cases (with ground slot or partial rectangular ground) have omnidirectional radiation patterns, as shown in the measured patterns of Fig. 10, taken at 4 GHz.

4. Antennas with reconfigurable band rejection

UWB technology is usually associated with the CR underlay mode [17]. It can, however, be implemented in the overlay mode. The difference between the two modes is the amount of transmitted power. In the underlay mode, UWB has a considerably restricted power, which is spread over a wide frequency band. In the overlay mode, however, the transmitted power can be much higher. It actually can be increased to a level that is comparable to the power

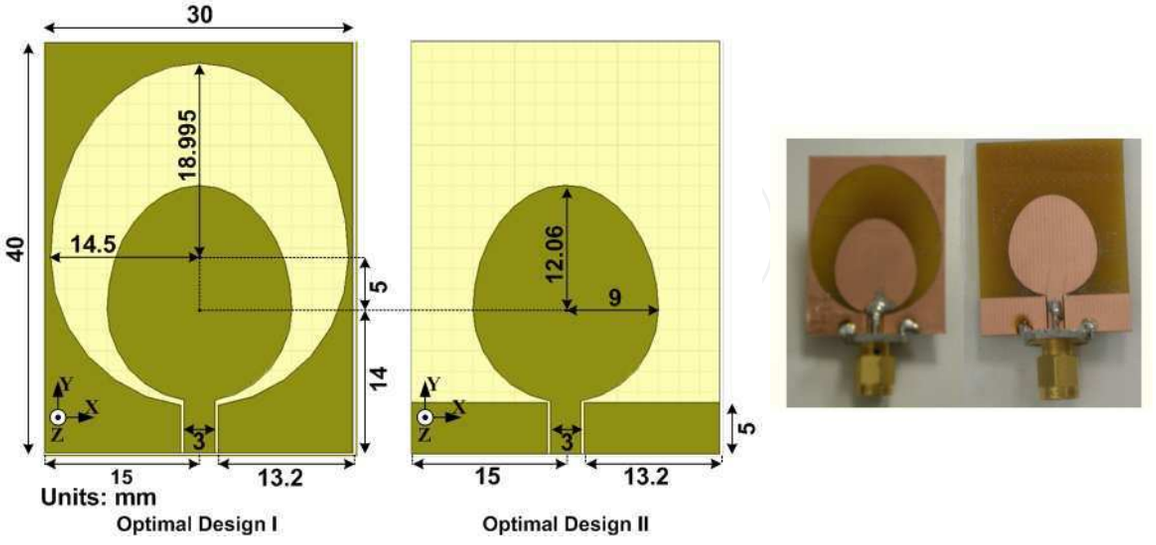
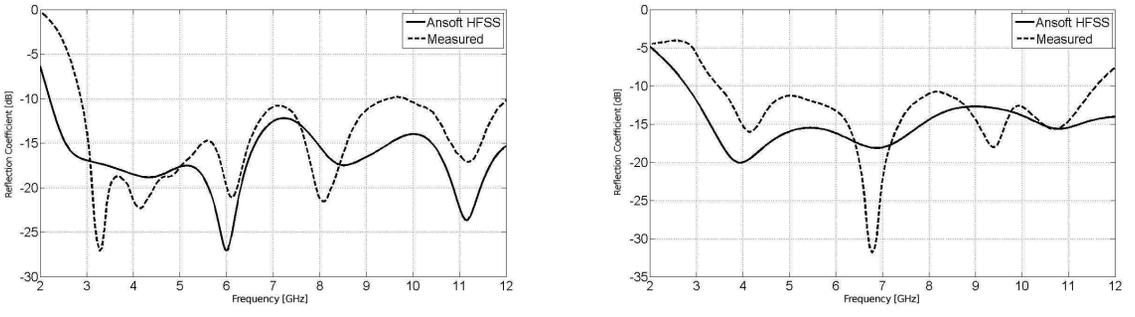


Figure 8. Two UWB antennas with optimized ground planes [14]



(a) Optimal Design I (b) Optimal Design II

Figure 9. Measured and computed reflection coefficients of the designs in Fig. 8

of licensed systems, which allows for communication over medium to long distances. But this mode is only applicable if two conditions are met: 1) if the UWB transmitter ensures that the targeted spectrum is completely free of signals of other systems, or shapes its pulse to have nulls in the bands used by these systems, and 2) if the regulations are revised to allow this mode of operation [18]. Pulse adaptation for overlay UWB CR has been discussed in [19]. UWB can also operate in both underlay and overlay modes simultaneously. This can happen by shaping the transmitted signal so as to make part of the spectrum occupied in an underlay mode and some other parts occupied in an overlay mode. In the overlay UWB scenario, the antenna at the front-end of the CR device should be capable of operating over the whole UWB range, for sensing and determining the bands that are being used by primary users, but should also be able to induce band notches in its frequency response to prevent interference to these users. Even if the UWB power is not increased, having these band notches prevent raising the noise floor of primary users.

http://dx.doi.org/10.5772/53430

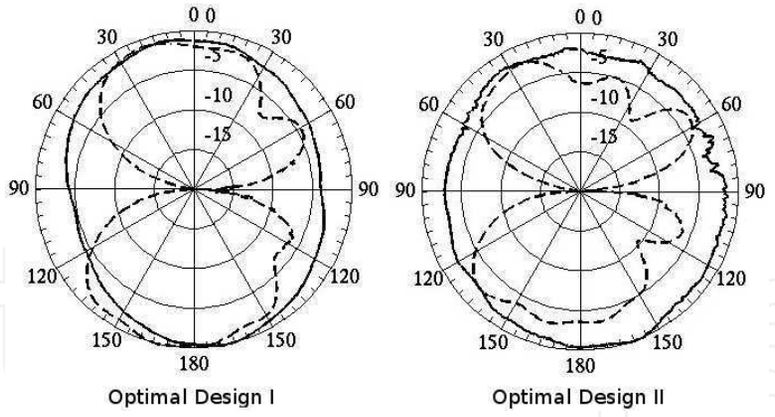


Figure 10. Measured radiation patterns of Optimal Design I (left column) and Optimal Design II (right column) in the XZ-plane (solid line) and the YZ-plane (dotted line) [14]

Antennas that allow the use of UWB in overlay CR are discussed in this Section. Several band-notching techniques are used in such antennas, the most famous of which being the use of split-ring resonators (SRRs) and the complementary split-ring resnators (CSRRs), which are discussed in 4.1. UWB antennas with fixed band notches are reported in [20–23]. Some UWB antennas with reconfigurable band notches, which are suitable for CR, are discussed below.

4.1. SRRs and CSRRs

Split-ring resonators (SRRs), originally proposed by Pendry *et al.* [24], have attracted great interest among electromagneticians and microwave engineers due to their applications to the synthesis of artificial materials (metamaterials) with negative effective permeability. From duality arguments, it has been shown that negative permittivity media can also be generated by means of resonant elements, namely, complementary split-ring resonators (CSRRs) [25]. These particles are simply the negative image of SRRs, and roughly behave as their dual counterparts.

The basic topologies of the SRR and the CSRR, and their equivalent-circuit models, are shown in Fig. 11. The equivalent-circuit models are reported in [26]. The SRR consists of two concentric metallic split rings printed on a microwave dielectric circuit board. The complementary of a planar metallic structure is obtained by replacing the metal parts of the original structure with apertures, and the apertures with metal plates. According to their lumped element models, SRRs and CSRRs do resonate. At the resonance frequency, SRRs have negative permeability, and CSRRs give negative permittivity, properties that lead to band rejection.

Single-ring SRRs and CSRRs are discussed in [27], where the relationship between the SRR and CSRR dimensions and their resonance frequencies are studied by simulations. The band rejection they cause about their resonance frequency can be controlled by mounting electronic switches across them and activating/deactivating these switches. This is illustrated in the example of Fig. 12, where two configurations of a reconfigurable bandstop filter are shown. In both configurations, a rectangular single-ring CSRR is incorporated in a 50-Ω microstrip line, which is printed on a 1.52mm-thick Rogers RO3203 substrate with $\varepsilon_r = 3.02$.

In the first configuration, an electronic switch (PIN diode or RF MEMS) is mounted on one side of the ring slot, as shown. Setting the switch ON leads to a resonating CSRR, which creates a stop band around the resonance frequency. When the switch is OFF, we end up with a complete unsplit ring, which does not have the characteristics of a CSRR, and as a result the stop band is removed. In the second configuration, a hard connection (or a capacitor with high capacitance) is present on one side of the ring slot, and a switch is mounted on the opposite side. When the switch is OFF, we have a CSRR with one gap, resonating at a certain frequency, and when the switch is ON, the CSRR will have two gaps, thus resonating at the higher frequency. The dimensions of the ring slot are chosen such that the stop band (of the single-gap case) is centered at 3.5 GHz. These dimensions are the same for both configurations.

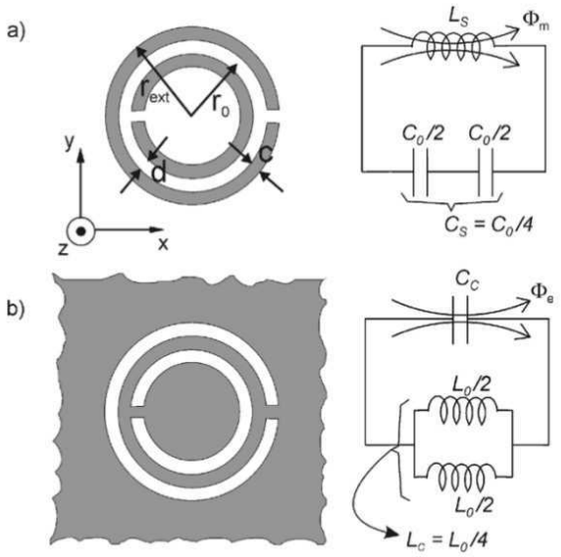
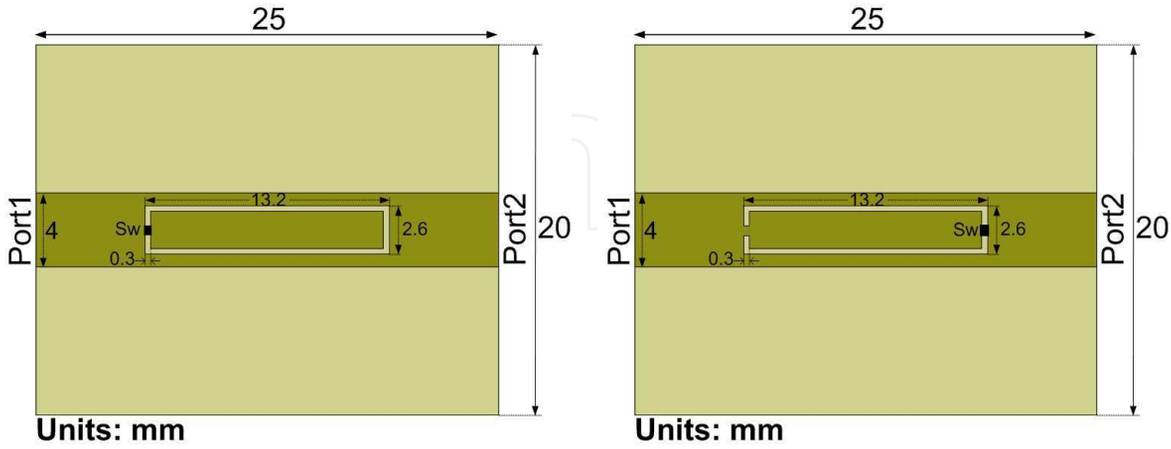


Figure 11. Topologies of the: (a) SRR and (b) CSRR, and their equivalent-circuit models. Grey zones represent the metallization. [26]



(a) Configuration 1 (b) Configuration 2

Figure 12. Reconfigurable bandstop filter based on a CSRR. (a) Configuration 1: electronic switch mounted over ring slot. (b) Configuration 2: hard connection on one side and an electronic switch over the CSRR slot on the other side.

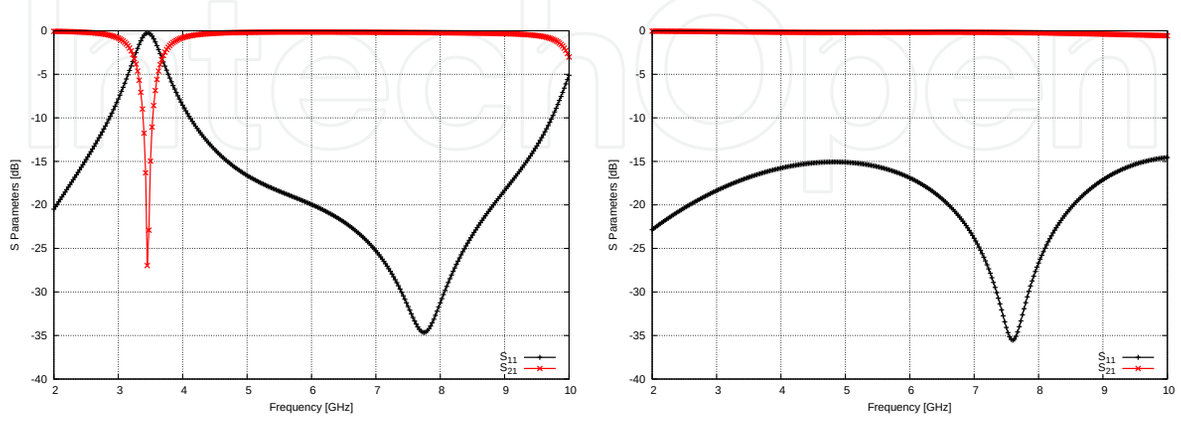
The computed reflection and transmission coefficients for the first configuration are shown in Fig. 13. For the switch-ON case, a stop band, centered at 3.5 GHz, is created (Fig. 13(a)). When the switch is OFF, the stop band disappears, and the all-pass behavior is retrieved (Fig. 13(b)). Fig. 14 plots the computed reflection and transmission coefficients for the second configuration. A stop band, centered at 3.5 GHz, results when the switch is OFF, as shown in Fig. 14(b). A narrower stop band is created at a higher frequency, 6.6 GHz, when the switch is ON (Fig. 14(a)). It is to note that theses result hold if the CSRR is instead incorporated in the ground plane below the microstrip line. Similar properties hold for SRRs, as reported in [27]. The switching components can be replaced with varactors, to obtain notch tunability.

4.2. Antennas with a single reconfigurable rejection band

The design of a UWB antenna with a single switchable band rejection is reported in [28]. Two inverted T-shaped slits are embedded on the ground plane to allow band rejection characteristic from 5 to 6 GHz, and a PIN diode is connected to each slit to enable the switching capability for this band rejection function.

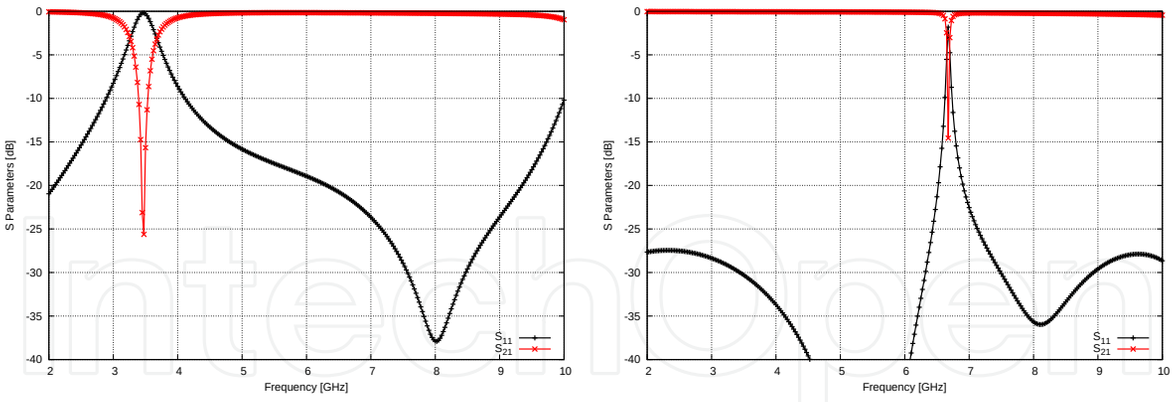
In [29], a wideband antenna with reconfigurable rejection within the operation band is presented. The antenna is a CPW-fed bow-tie, where a slot etched along the bow-tie upper edge provides the rejection of a certain band. Six PIN diodes mounted across the slots are used as switching elements, but only four switching cases are of use: one results in a notch-free wideband response, and the remaining three result each in a rejection in separate bands.

A UWB design with a single reconfigurable band notch is proposed in [30]. The configuration of this design and a photo of its fabricated prototype are shown in Fig. 15. Originally, the antenna is a UWB monopole, printed on a $30 \times 30 \times 1.6$ mm^3 Rogers RO3006 substrate with a dielectric constant $\varepsilon_r = 6.15$. It has a microstrip line feed and a partial ground plane. The patch is rectangular and is 14 mm $\times$ 15.5 mm in size, the ground is 30 mm $\times$ 10 mm, and the feed line is 2.4 mm $\times$ 10.5 mm. For better matching, the corners of the patch are rounded, by intersecting it with a circle of radius 8.75 mm, and a slit is etched in the ground below the



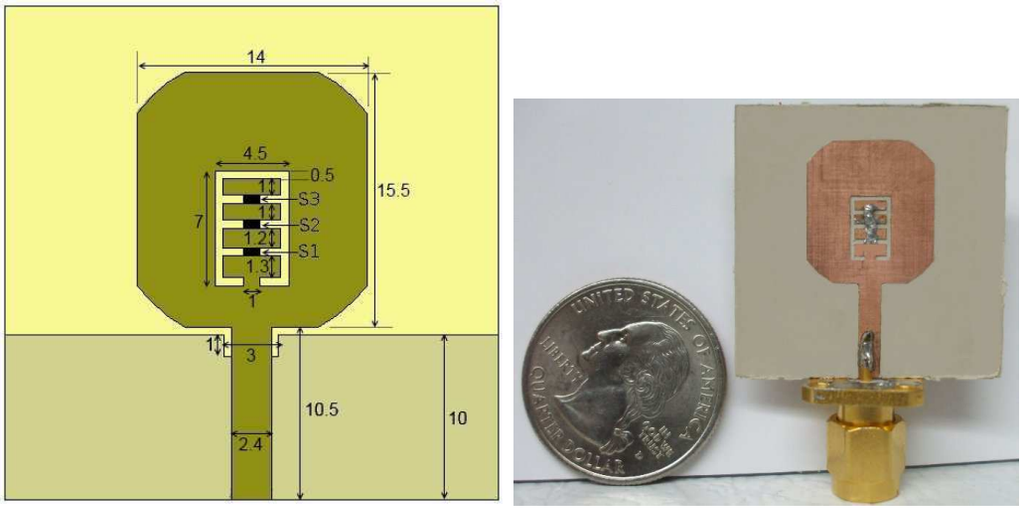
(a) Switch ON (b) Switch OFF

Figure 13. Reflection coefficient and transmission of CSRR-based filter in Fig. 12(a). (a) Switch is ON. (b) Switch is OFF.



(a) Switch OFF (b) Switch ON

Figure 14. Reflection coefficient and transmission of CSRR-based filter in Fig. 12(b). (a) Switch is OFF. (b) Switch is ON.

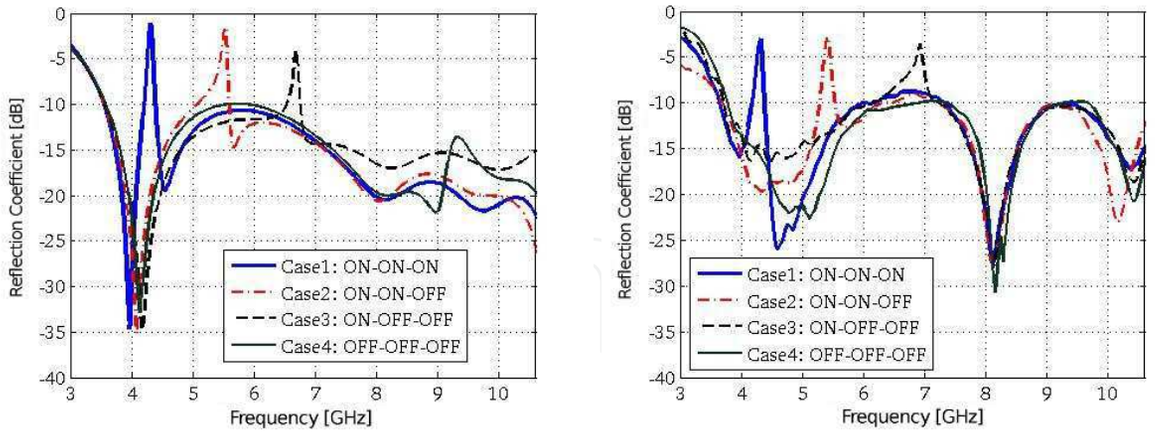


(a) (b)

Figure 15. Configuration and photo of an antenna with one reconfigurable rejection band [30]

feed. The slit is 3 mm $\times$ 1 mm. As a result, this antenna has an impedance bandwidth that covers the whole UWB frequency range. Four nested CSRRs are incorporated in the patch. Three electronic switches, 1mm$\times$0.5mm in size, are mounted across the slots. The sequential activation (deactivation) of the switches leads to the functioning of a larger (smaller) CSRR, and thus results in a notch at a lower (higher) frequency. The following switching cases are considered: Case 1 when all three switches are ON, Case 2 when only S3 is deactivated, Case 3 when only S1 is ON, and finally Case 4 when all switches are OFF. The resulting reflection coefficient plots, corresponding to the different switching states, are shown in Fig. 16. The plots show one notch, which can occur in one of 3 bands, or can completely disappear. In the latter case, the antenna retrieves its UWB response, which enables it to sense the whole UWB range.

http://dx.doi.org/10.5772/53430

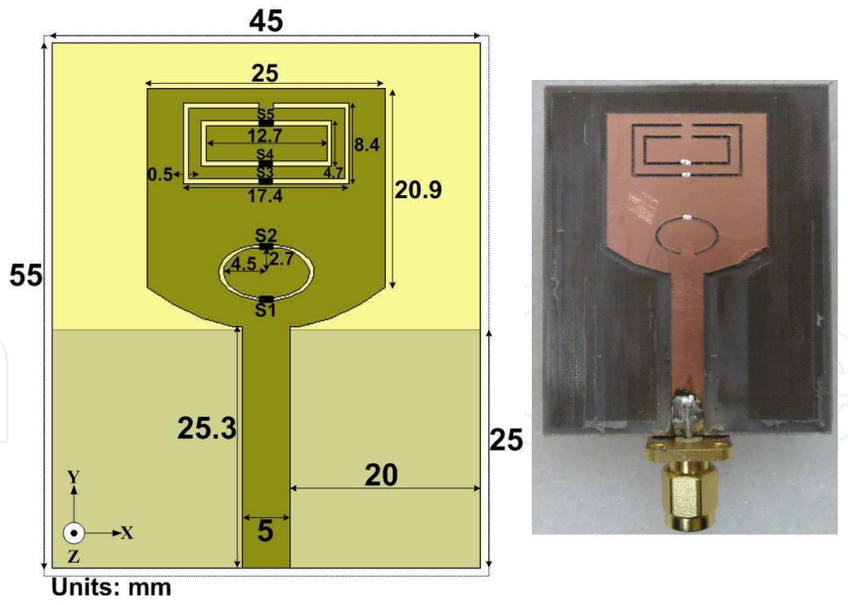


(a) Computed (b) Measured

Figure 16. Computed and measured reflection coefficient for the different switching cases of the antenna in Fig. 15

4.3. Antennas with multiple reconfigurable rejection bands

The antenna reported in [31] is capable of inducing three band notches, which are independently controllable, using only three RF switches. Illustrated in Fig. 17, the antenna is a monopole printed on a 1.6-mm-thick Taconic TLY substrate with $\varepsilon_r = 2.2$, and features a partial rectangular ground plane. The patch is rectangular in shape, but the corners of the rectangle around the feed line are rounded to create a matching section. The dimensions of the different parts are optimized for an impedance bandwidth covering the 2–11 GHz range.



(a) (b)

Figure 17. (a) Configuration of a UWB antenna with three independently reconfigurable band notches, and (b) photo of its prototype [31]

To create the band notches, two rectangular and one elliptical CSRRs are etched on the patch. Their shapes are selected to suit the part of the patch they are fitted in. Their sizes

Case	Notch bands (GHz)	S1	S2	S3
1	None (UWB operation)	ON	ON	ON
2	2.4	ON	OFF	ON
3	3.5	ON	ON	OFF
4	5.2	OFF	ON	ON
5	2.4, 3.5	ON	OFF	OFF
6	2.4, 5.2	OFF	OFF	ON
7	3.5, 5.2	OFF	ON	OFF
8	2.4, 3.5, 5.2	OFF	OFF	OFF

Table 1. The 8 switching cases for the design in Fig. 17 and the corresponding notched bands.

are optimized so that the larger rectangular CSRR causes a notch in the 2.4 GHz band, the smaller one in the 3.5 GHz band, and the elliptical one in the 5.2 GHz band. To enable band notch reconfigurability, three electronic switches (S1, S2, and S3) are mounted across the CSRRs.

The state of a switch controls the notch causing by the corresponding CSRR. When S1 is OFF, the elliptical CSRR induces a notch in the 5.2 GHz band. When S2 is OFF, the large rectangular CSRR causes a notch in the 2.4 GHz band. For the smaller rectangular CSRR, a notch appears at 3.5 GHz when S3 is OFF. When a switch is ON, the corresponding CSRR behaves as one with two gaps, and its resonance moves up in frequency and becomes too weak to affect the UWB response of the antenna. The different switching cases lead to different band notch combinations. These include the scenarios of one, two, three concurrent notches, or no notch at all. In the latter case, the antenna has a UWB response, which is required for channel sensing.

There are eight possible switching scenarios for this antenna, which are listed in Table 1. Fig. 18 shows the computed and measured reflection coefficient plots for some of the switching cases. For Case 1, a UWB response is obtained. The results for Case 2 reveal a single notch in the 2.4 GHz band, those for Case 4 show a single notch in the 5.2 GHz band, the results for Case 5 show two notches in the 2.4 and 3.5 GHz bands, and those for Case 8 show three notches in the 2.4, 3.5, and 5.2 GHz bands. A notch in a certain band helps to prevent interference to a primary user or the service operated in that band.

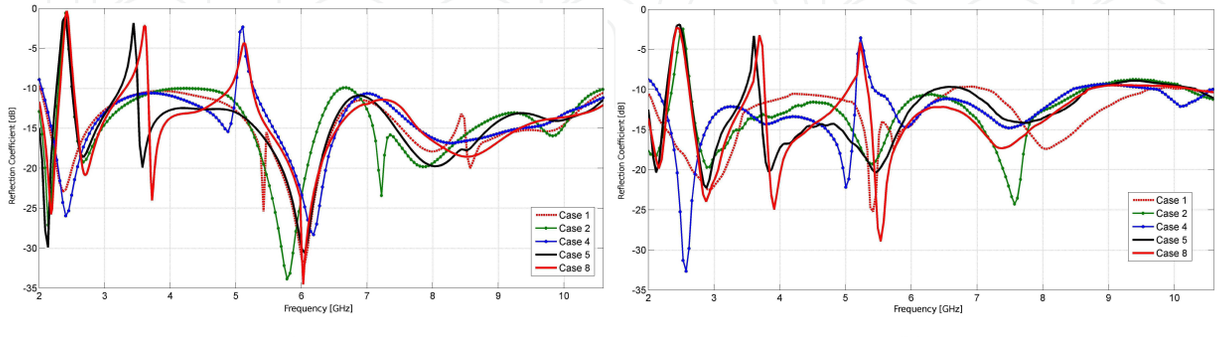
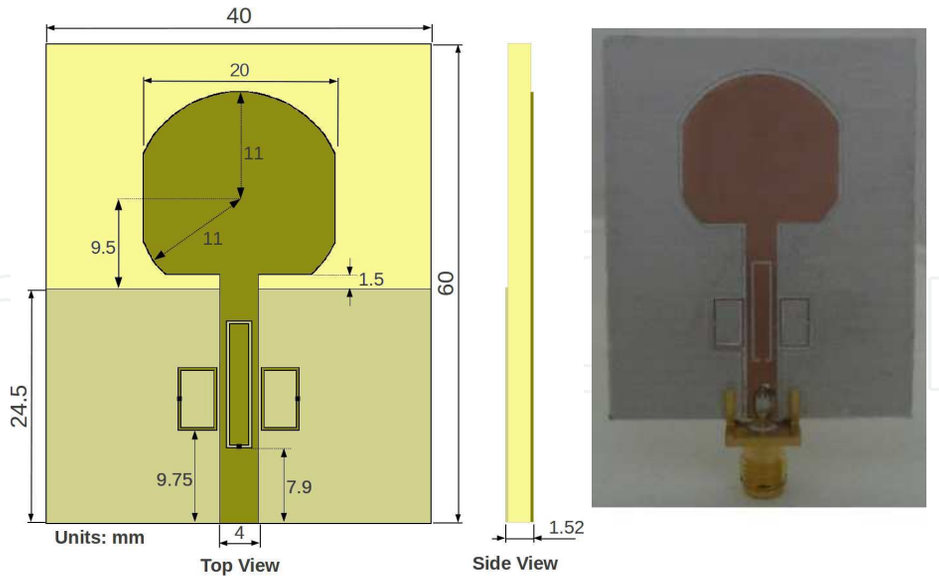


Figure 18. (a) Simulated and (b) measured reflection coefficient plots for the antenna in Fig. 17 for some of the adopted switching cases

http://dx.doi.org/10.5772/53430



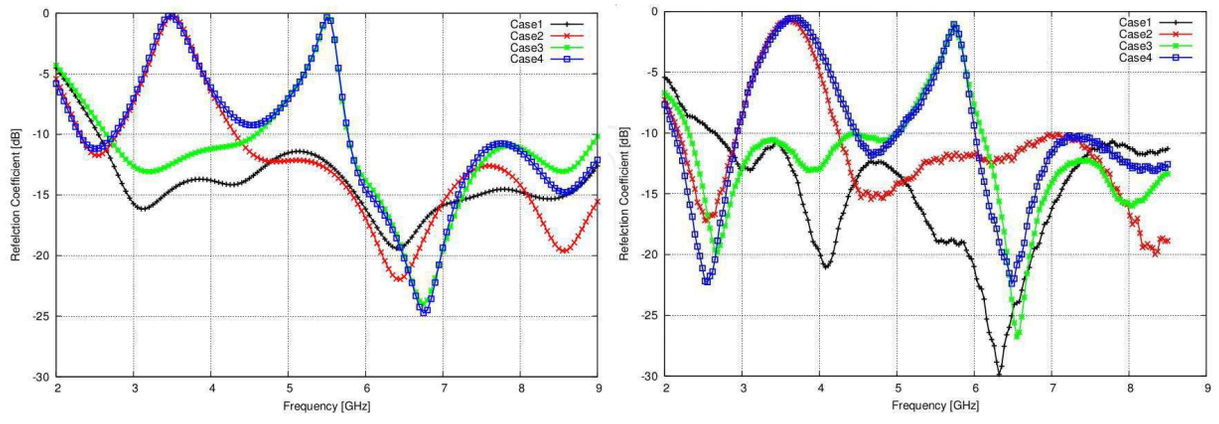
(a) (b)

Figure 19. (a) Configuration of a filter antenna with two reconfigurable band notches, and (b) photo of its prototype [32]

The antenna has omnidirectional radiation patterns. It also has good gain values in its band(s) of operation. In a notched band, the gain drops to negative values due to strong reflections at the antenna's port.

4.4. Filter antennas with reconfigurable band notches

A UWB antenna with reconfigurable band notches can be designed by incorporating a bandstop filter in the feed line of a UWB antenna. With this structure, the switching elements will be mounted on the feed line, away from the radiating patch, which makes the bias circuit simpler to design.



(a) (b)

Figure 20. (a) Simulated and (b) measured reflection coefficient plots for the antenna in Fig. 19 for the four adopted switching cases.

A filter antenna with two reconfigurable rejection bands is presented in [32]. Its structure is shown in Fig. 19. The UWB antenna is based on a rounded patch and a partial rectangular

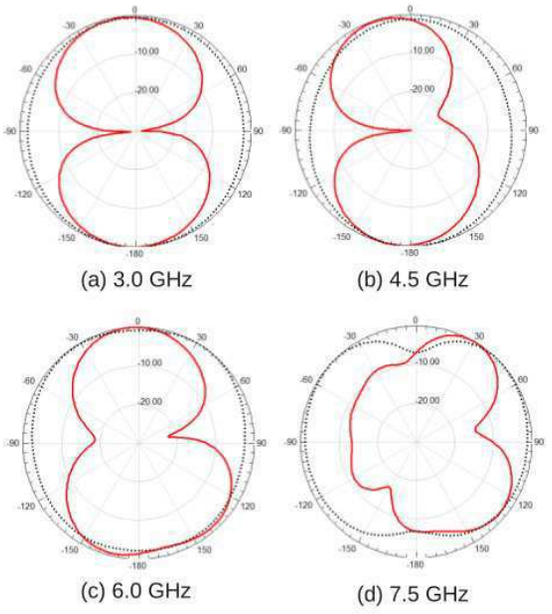


Figure 21. Radiation patterns of the antenna in Fig. 19 in the H-plane (dotted line) and E-plane (solid line)

ground plane. The Rogers RO3203 material is used for the 1.52mm-thick substrate. A reconfigurable filter with two stop bands is incorporated along its microstrip feed line. The filter is based on one rectangular single-ring CSRR etched on the line, and two identical rectangular single-ring SRRs placed in close proximity to it. The resonance of the CSRR is controlled via a switch, and that of the two SRRs via two switches that are operated in parallel. As a result, there are four switching scenarios. The simulated and measured S_{11} plots are shown in Fig. 20. Case 1, where no band notches exist, allows the antenna to sense the UWB range to determine the narrowband primary services that are transmitting inside the range. In the other three cases, the notches block the UWB pulse components in the 3.5 GHz band, the 5.5 GHz band, or both. It should be noted that notches due to the SRRs and the CSRR around the feed are stronger than those due to CSRRs or any notching structures implemented in the patch. This is because energy is concentrated in a smaller area in the feed, and coupling with the SRRs/CSRR is higher.

The normalized gain patterns of the filter antenna, for Case1, are shown in Fig. 21. The antenna has good omnidirectional patterns, and this is expected since its is a printed monopole with a small ground plane not covering the radiating patch. Since the patch is untouched, the patterns are independent of the switching cases. The realized peak gain of the antenna is plotted in Fig. 22 for Case 1 and Case 4. In Case 4, the gain drops sharply, to below -10 dB, at 3.5 GHz and at 5.5 GHz. In these two bands, very high reflections occur at the antenna's input. The gain drop in the notch band is large, as the coupling the CSRR and the SRRs cause is high. Due to the location of the switches, connecting the DC bias lines, especially to the SRRs, which are DC-separated from anything else, is an easy task. A wire can be used to drive the switch on the CSRR. A note is that extra band notches can be obtained by placing more SRRs around the feed line.

http://dx.doi.org/10.5772/53430

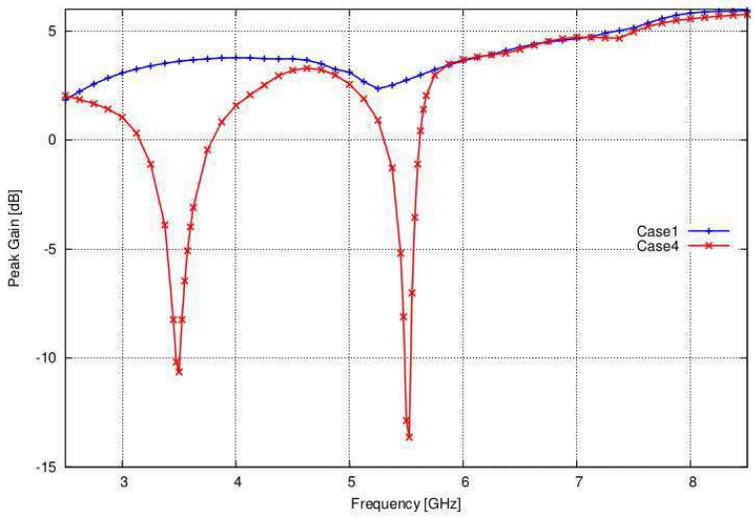


Figure 22. Realized peak gain of the antenna in Fig. 19. Case 1: gain is positive. Case 4: gain is negative in the 3.5 and 5.5 GHz bands.

5. Antennas for overlay CR

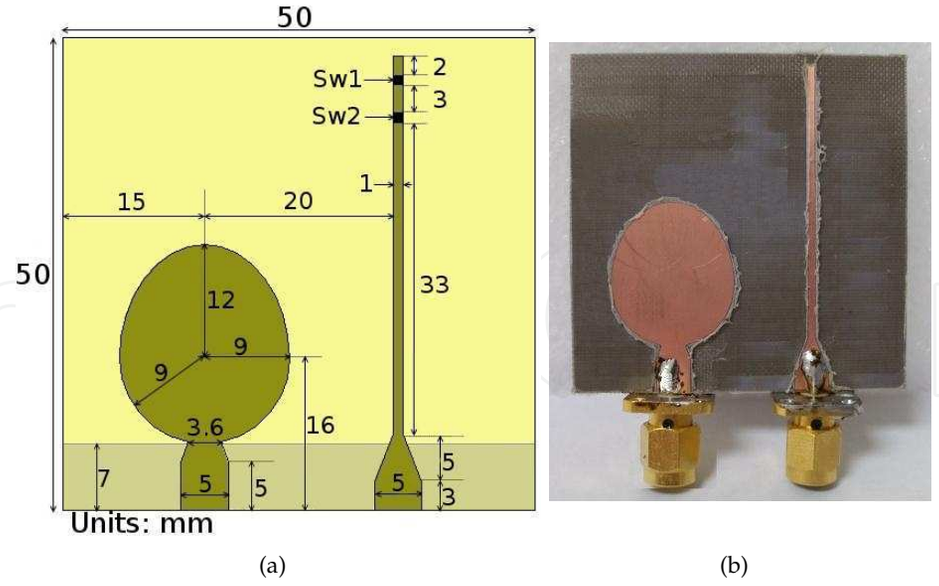
Antennas designed for overlay CR should have the capability to sense the channel and communicate over a small portion of it. These antennas can be implemented as dual-port, where one port is UWB, and the other is narrowband and frequency reconfigurable. The design of UWB antennas was discussed in Section 3. They can also be designed as single-port, where the same port is used for both sensing and communicating, and thus should switch between wideband and narrowband operations. The advantages of each design will be revealed in the rest of this Section.

5.1. Dual-port antennas for overlay CR

A dual-port antenna for overlay was proposed by Ebrahimi *et al.* [33, 34]. The structure consists of two printed antennas namely a wide- and a narrow-band antenna. Because the two antennas are in close proximity, high coupling exists between them, and the patterns of the NB antenna are affected by the presence of the UWB one. The authors successfully designed modified versions of the antenna system to solve the coupling issue.

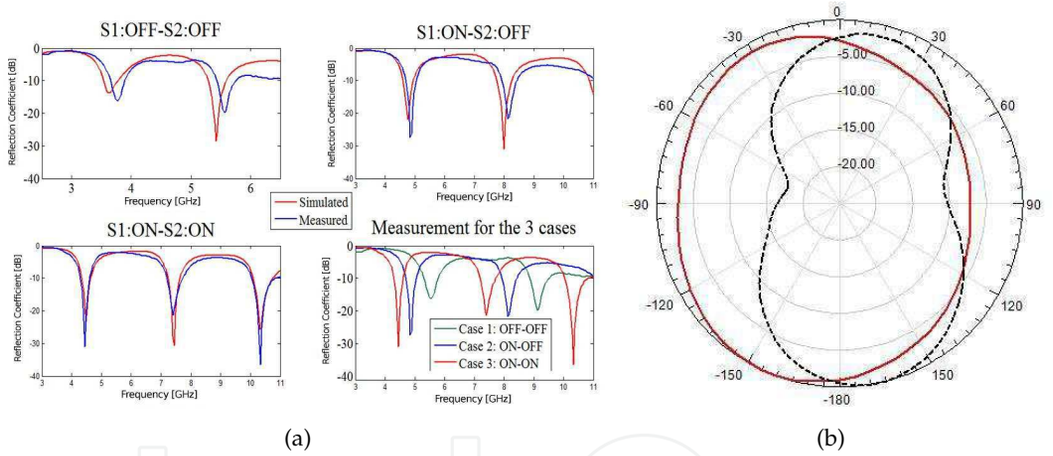
A simpler design that offers good isolation between the two antenna ports is presented in [35]. The configuration of this design, which comprises two microstrip-line-fed monopoles sharing a common partial ground, is shown in Fig. 23. The sensing UWB antenna is based on an egg-shaped patch, obtained by combining a circle and an ellipse at their centers. A small tapered microstrip section is used to match the 50-Ω feed to the input impedance of the patch. The UWB response of the sensing antenna is guaranteed by the design of the patch, the partial ground plane, and the feed matching section. The reflection coefficient of the sensing antenna, and its normalized 5-GHz patterns, are shown in Fig. 24.

The communicating antenna is a microstrip line connected to a 50-Ω feed line via a matching section. Two electronic switches are incorporated along this line. By controlling the switches, the length of the antenna is changed, which leads to various resonance frequencies inside the UWB range. Three switching cases are considered: Case 1 where both switches are deactivated, Case 2 where Switch 1 is ON and Switch 2 is OFF, and Case 3 where both



(a) (b)

Figure 23. Dual-port UWB-NB antenna for overlay CR (a) configuration and (b) photo of a fabricated prototype [35]



(a) (b)

Figure 24. (a) Reflection coefficient of the sensing UWB antenna, and (b) its normalized gain patterns at 5 GHz: H-plane (solid line) and the E-plane (dashed line) [35]

switches are activated. The resulting measured reflection coefficient plots are given in Fig. 25, which shows clear frequency reconfigurability and coverage of most of the UWB range.

The transmission S_{21} at the resonance frequencies, for the three switching cases, are given in Table 2. Good isolation between the UWB and NB port is achieved, given the simplicity of the design.

	Case 1		**Case 2**		**Case 3**		
f (GHz)	5.55	9.15	4.85	8.15	4.44	7.41	10.33
S_{21} (dB)	-31.4	-14.8	-16.8	-15.5	-21.3	-22.6	-15.7

Table 2. Transmission S_{21} for the design in [35]

http://dx.doi.org/10.5772/53430

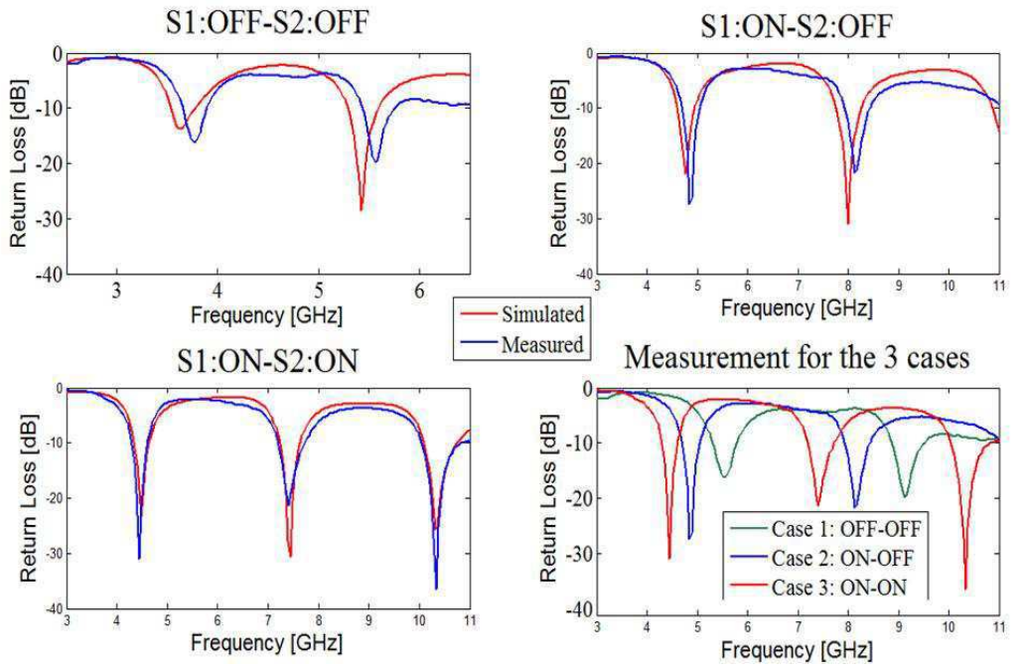


Figure 25. Measured reflection coefficient of the communicating antenna [35]

The communicating antenna has also omnidirectional patterns, but some degradation occurs due to the presence of the UWB patch.

5.2. Single-port antennas for overlay CR

Dual-port antennas enable simultaneous sensing and communicating over the channel, but have limitations in terms of their relatively large size, the coupling between the two ports, and the degraded patterns. These limitations are solved by the use of single-port antennas, but these are only suitable when the channel does not change very fast, and thus sensing and communication are possible, sequentially. Single-port CR antennas are also more challenging to design.

A reconfigurable wideband/dual-band double C-slot microstrip patch antenna is proposed in [36]. The frequency tuning is performed by switching ON and OFF two patches. The antenna operates in one of two different dual-band modes when either patch is activated, and in very wide band mode when both patches are excited.

In [37], a single-port Vivaldi antenna with added switched band functionality to operate in a wideband or narrowband mode is presented. Frequency reconfigurability in this design is attained by inserting four pairs of ring slots into the structure, and switching them using PIN diodes. A wide bandwidth mode covering the 1.0–3.2 GHz range, and three narrowband modes within this range, can be selected. A single pair of ring slots, and fifteen PIN diode switches across, are used on the single-port Vivaldi design in [38]. For this antenna, a wideband operation is obtained over the 1–3 GHz band, inside which there are six narrowband states of use. In these two Vivaldi antenna designs, the switching elements, PIN diodes in this case, are mounted on the radiating parts of the antennas. This makes the design of the DC bias circuits a complex task, as the designers have to make sure these circuits have little interference to the antenna performance.

The single-port overlay CR antenna in [39] has the switching elements mounted along its microstrip feed line, away from the radiating patch. This property has the advantage that the DC bias circuit causes limited interference to the antenna characteristics. The antenna is initially UWB, which makes it sensing-capable. A reconfigurable bandpass filter is then embedded along its feed line. When activated, the filter can transform the UWB frequency response into a reconfigurable narrowband one, which is suitable for the communication operation of the CR system. The configuration of the antenna, and a closer view of its embedded filter part, are shown in Fig. 26. It features a partial rectangular ground plane, a rectangular patch, and a curved matching section between the microstrip feed line and the patch. The filter is based on a symmetrical defected microstrip structure (DMS) implemented in the feed line of the UWB antenna. It has a T-shaped slot, which by itself, has bandstop characteristics. However, when placed between a pair of gaps, which act as capacitors, a bandpass structure results [40].

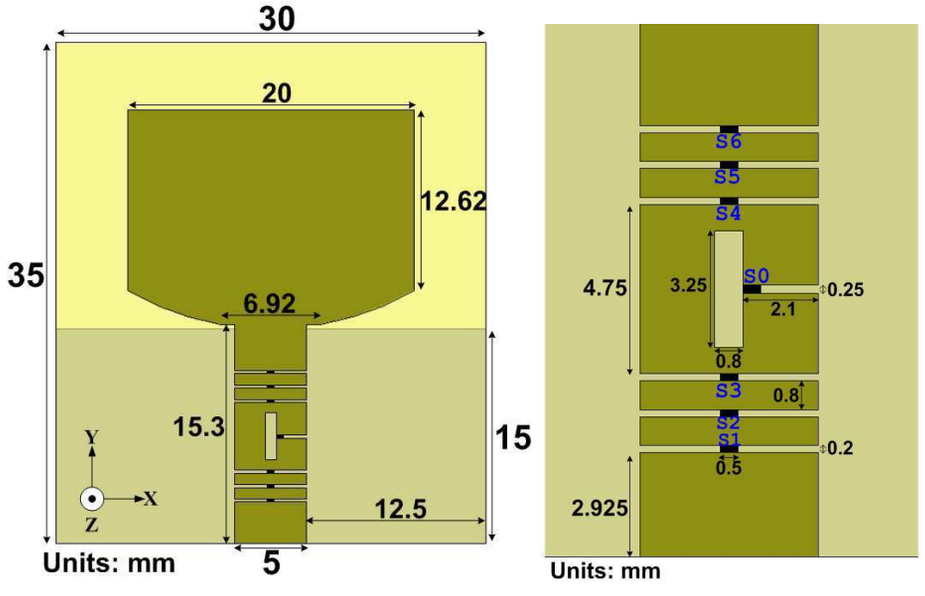


Figure 26. A reconfigurable UWB/NB filter antenna. (a) Configuration, and (b) closer view of the embedded filter [39]

For the purpose of achieving frequency reconfigurability, three pairs of gaps are symmetrically placed around the T-slot, and seven electronic switches are placed across the slots as shown. Six switching cases are considered, as indicated in Table 3. Case 0 corresponds to all the switches being ON. In this case, the effect of the filter is canceled, bringing back the UWB response of the antenna. The frequency characteristics of the filter depend on the dimensions of the slots, and on the switching state.

The computed and measured reflection coefficient plots for the six switching cases are given in Fig. 27. The operation of the antenna makes it suitable for employment in cognitive radio applications, where Case 0 could be used for sensing the channel (to determine the white spaces), and the other cases for communicating in the corresponding white space. Further resonances can be obtained by including more gaps around the T-slot and appropriately choosing their locations and widths.

http://dx.doi.org/10.5772/53430

Case	Switches in OFF state
0	None (all ON)
1	S0, S1, S6
2	S0, S1, S5
3	S0, S2, S5
4	S0, S3, S5
5	S0, S3, S4

Table 3. The six adopted switching cases for the single-port design in [39]

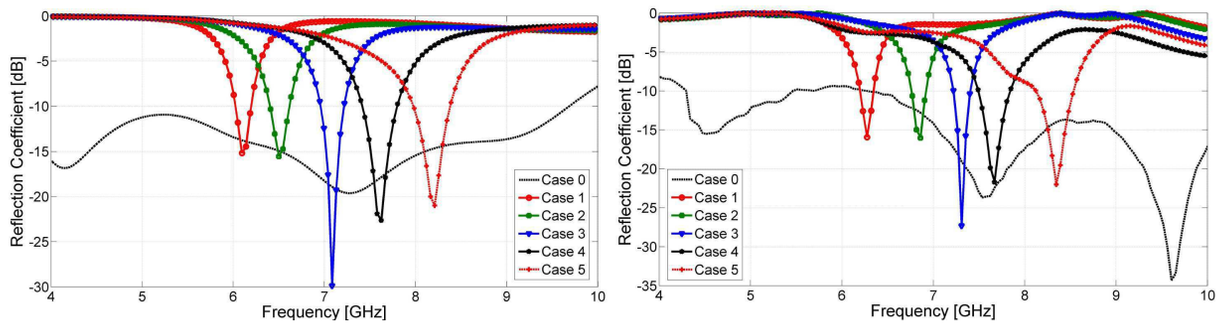


Figure 27. (a) Simulated, and (b) measured reflection coefficient [39]

5.3. A Single-port tunable filter antenna for overlay CR

Reconfigurable NB antennas can operate over a limited number of bands inside a designated frequency range. Tunable antennas, on the other hands, can be reconfigured to resonate at theoretically an infinite number of frequencies within a certain band. Tunable antennas can be used for communicating in a CR system, by tuning to a white space. They can also be employed for channel sensing, by progressively scanning small portions of the band. This depends of course on the rate at which the channel is changing, and on the tuning speed.

A tunable filter antenna is shown in Fig. 28. The initially UWB design features a tunable bandpass filter embedded along its microstrip feed line. It has a rounded patch and a partial rectangular ground plane. The Rogers RO3203 material, with $\varepsilon_r = 3.02$, is used for the 1.52mm-thick substrate. The filter is based on a T-shaped slot incorporated in the microstrip line between a pair of gaps.

For the purpose of achieving frequency tunability, a varactor is included in the design, as indicated. Changing the capacitance of the varactor changes the notch band caused by the T-slot, and as a result the narrow pass band of the overall filter. The DC lines of the varactors are connected with ease. Due to the presence of the two gaps, DC is separated from both the antenna port and the patch. Two surface-mount inductors are used over the DC lines as RF chokes. The reflection coefficient plots, obtained in Ansoft HFSS, are given in Fig. 29. They show narrowband tunability over the 4.5–7 GHz frequency range, for capacitance values between 0.3 and 7 pF.

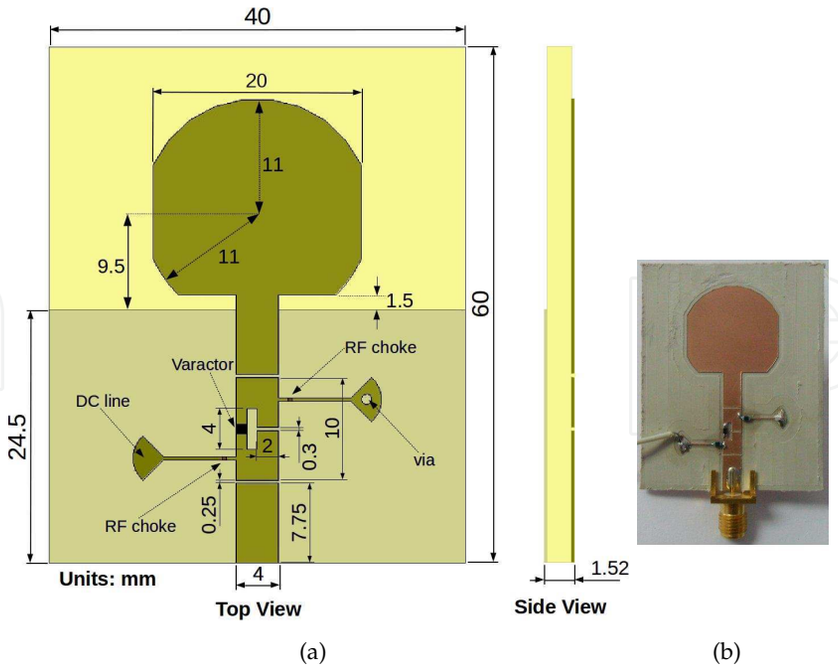


Figure 28. (a) Configuration of a tunable filter antenna, and (b) photo of a fabricated prototype. This antenna has a tunable bandpass filter embedded along its feed line.

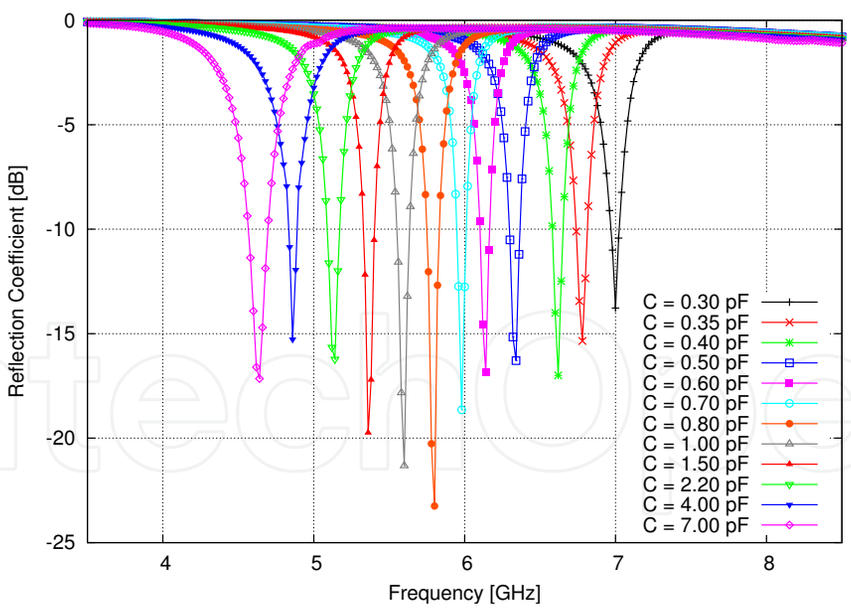


Figure 29. Reflection coefficient of the tunable filter antenna. Narrowband tunability is achieved

A UWB operation of the antenna can be made possible by installing 3 switching elements (e.g. PIN diodes) across the T-shaped slot and the two gaps. When these switches are ON, the effect of the narrowband bandpass filter is canceled, and the original UWB response of the antenna is retrieved. Tunablility would still be possible by putting the switches to the OFF state and adjusting the varactor capacitance. Extra DC biasing lines are required to

control the switches, but they will be installed away from the radiating patch. This makes their design relatively simple.

6. Summary

This chapter has discussed the design of antennas for Cognitive Radio applications. CR is a revolutionary spectrum allocation technology that allows unlicensed users to access spectrum bands licensed to primary users, at the condition of avoiding interference to them. Spectrum underlay and spectrum overlay are two approaches to sharing spectrum between primary and secondary users.

UWB antennas are required for sensing in overlay CR, and for communicating in underlay CR. Modified UWB antennas with reconfigurable band notches allow to employ UWB technology in overlay CR and to achieve high-data-rate and long distances communications. Overlay CR requires reconfigurable wideband/narrowband antennas, to perform the two tasks of sensing a wide band and communicating over a narrow white space. UWB antennas, antennas with reconfigurable band rejections, and single-port/dual-port wide-narrowband and tunable antennas suitable for these approaches have been reported.

Author details

Mohammed Al-Husseini[1], Karim Y. Kabalan[1],
Ali El-Hajj[1] and Christos G. Christodoulou[2]

1 American University of Beirut, Lebanon
2 University of New Mexico, USA

References

[1] Federal Communications Commission (2002) Spectrum Policy Task Force Report, Technical Report.

[2] Chen K.-C, Prasad R. (2009) Cognitive Radio Networks. ISBN 978-0-470-69689-7. West Sussex, United Kingdom: John Wiley & Sons.

[3] Zhao Q, Sadler B.M (2007) A Survey of Dynamic Spectrum Access: Signal Processing, Networking, and Regulatory Policy. IEEE signal processing magazine. 24:3:79–89.

[4] Low Z.N, Cheong J.H, Law, C.L (2005) Low-cost PCB Antenna for UWB Applications. IEEE antennas and wireless propagation letters. 4:237–239.

[5] Mehdipour A, Mohammadpour-Aghdam K, Faraji-Dana R, Kashani-Khatib M.-R (2008) A Novel Coplanar Waveguide-fed Slot Antenna for Ultra- wideband Applications. IEEE transactions on antennas and propagation. 56:12:3857–3862.

[6] Oraizi H, Hedayati S (2011) Miniaturized UWB Monopole Microstrip Antenna Design by the Combination of Giusepe Peano and Sierpinski Carpet Fractals. IEEE antennas and wireless propagation letters. 10:67–70.

[7] Azari A (2011) A New Super Wideband Fractal Microstrip Antenna. IEEE transactions on antennas and propagation. 59:5:1724–1727.

[8] Ghaderi M.-R, Mohajeri F (2011) A Compact Hexagonal Wide-slot Antenna with Microstrip-fed Monopole for UWB Application. IEEE antennas and wireless propagation letters. 10:682–685.

[9] Liu W, Yin Y, Xu W, Zuo S (2011) Compact Open-slot Antenna with Bandwidth Enhancement. IEEE antennas and wireless propagation letters. 10:850–853.

[10] Al-Husseini M, Ramadan A, El-Hajj A, Kabalan K.Y (2008) A 1.9-13.5 GHz Low-cost Microstrip Antenna. Proceedings of the 2008 International Wireless Communications and Mobile Computing Conference (IWCMC 2008). Crete Island, Greece. 6–8 Aug 2008.

[11] Al-Husseini M, Ramadan A, El-Hajj A, Kabalan K.Y (2009) Design of a Compact and Low-cost Fractal-based UWB PCB Antenna. Proceedings of the 26th National Radio Science Conference (NRSC 2009). Cairo, Egypt. 17–19 Mar 2009.

[12] Al-Husseini M, Tawk Y, El-Hajj A, Kabalan K.Y (2009) A Low-cost Microstrip Antenna for 3G/WLAN/WiMAX and UWB Applications. Proceedings of the 2009 International Conference on Advances in Computational Tools for Engineering Applications (ACTEA 2009). Zouk Mosbeh, Lebanon. 15–17 Jul 2009. pp. 68–70.

[13] Al-Husseini M, Ramadan A, Tawk Y, El-Hajj A, Kabalan, K.Y (2009) Design and Ground Plane Consideration of a CPW-fed UWB Antenna. Proceedings of the 2009 International Conference on Electrical and Electronics Engineering (ELECO 2009). Bursa, Turkey. 5–8 Nov 2009. pp. II-151–II-153.

[14] Al-Husseini M, Ramadan A, Tawk Y, El-Hajj A, Kabalan, K.Y (2011) Design and Ground Plane Optimization of a CPW-fed UWB Antenna. Turkish journal of electrical engineering and computer sciences. 19:2:243–250.

[15] Curto S, John M, Ammann M (2007) Groundplane Dependent Performance of Printed Antenna for MB-OFDM-UWB. Proceedings of the IEEE 65th Vehicular Technology Conference. Dublin, Ireland. 22–25 Apr 2007. pp. 352–356.

[16] OOi P.C, Selvan K.T (2010) The Effect of Ground Plane on the Performance of a Square Loop CPW-fed Printed Antenna. Progress in electromagnetics research letters. 19:103–111.

[17] Arslan H, Sahin M (2007) UWB-based Cognitive Radio Networks. In: Hossain E, Bhargava V, editors. Cognitive Wireless Communication Networks. US: Springer.

[18] Zhang H, Zhou X, Chen T (2009) Ultra-wideband Cognitive Radio for Dynamic Spectrum Accessing Networks. In: Xiao Y, Hu F, editors. Cognitive Radio Networks. ISBN 978-1-4200-6420-9. Boca Raton, Florida: CRC Press. pp. 353–382.

[19] Safatly L, Al-Husseini M, El-Hajj A, Kabalan K.Y (2012) Advanced Techniques and Antenna Design for Pulse Shaping in UWB Cognitive Radio. International journal of antennas and propagation. DOI:10.1155/2012/390280.

[20] Kelly J.R, Hall P.S, Gardner P, (2011) Band-notched UWB Antenna Incorporating a Microstrip Open-loop Resonator. IEEE transactions on antennas and propagation. 59:8:3045–3048.

[21] Nguyen T.-D, Lee D.-H, Park H.-C (2011) Design and Analysis of Compact Printed Triple Band-notched UWB Antenna. IEEE antennas and wireless propagation letters. 10:403–406.

[22] Almalkawi M, Devabhaktuni V (2011) Ultrawideband Antenna with Triple Band-notched Characteristics Using Closed-loop Ring Resonators. IEEE antennas and wireless propagation letters. 10:959–962.

[23] Kim D.-O, Jo N.-I, Jang H.-A, Kim C.-Y (2011) Design of the Ultrawideband Antenna with a Quadruple-band Rejection Characteristics Using a Combination of the Complementary Split Ring Resonators. Progress in electromagnetics research, 112:93–107.

[24] Pendry J.B, Holden A.J, Robbins D.J, Stewart W.J (1999) Magnetism from Conductors and Enhanced Nonlinear Phenomena. IEEE transactions on microwave theory and techniques. 47:11:2075–2084.

[25] Falcone F, Lopetegi T, Laso M.A.G, Baena J.D, Bonache J, Beruete M, Marques R, Martin F, Sorolla M (2004) Babinet Principle Applied to the Design of Metasurfaces and Metamaterials. Physical review letters. 93:19:197401-1–197401-4.

[26] Baena J.D *et al.* (2005) Equivalent-circuit Models for Split-ring Resonators and Complementary Split-ring Resonators Coupled to Planar Transmission Lines. IEEE transactions on microwave theory and techniques. 53:4:1451–1461.

[27] Al-Husseini M (2012) Antenna Design for Overlay and Underlay Cognitive Radio Applications, Ph.D. Dissertation. Beirut, Lebanon: American University of Beirut.

[28] Sim C.-Y.-D, Chung W.-T, Lee C.-H (2010) Planar UWB Antenna with 5 GHz Band Rejection Switching Function at Ground Plane. Progress in electromagnetics research. 106:321–333.

[29] Perruisseau-Carrier J, Pardo-Carrera P, Miskovsky P (2010) Modeling, Design and Characterization of a Very Wideband Slot Antenna with Reconfigurable Band Rejection. IEEE transactions on antennas and propagation. 58:7:2218–2226.

[30] Al-Husseini M, Costantine J, Christodoulou C.G, Barbin S.E, El-Hajj A, Kabalan, K.Y (2010) A Reconfigurable Frequency-notched UWB Antenna with Split-ring Resonators. Proceedings of the 2010 Asia-Pacific Microwave Conference (APMC 2010). Yokohama, Japan. 7–10 Dec 2010.

[31] Al-Husseini M, Ramadan A, Tawk Y, Christodoulou C.G, El-Hajj A, Kabalan K.Y (2011) Design Based on Complementary Split-ring Resonators of an Antenna with Controllable Band Notches for UWB Cognitive Radio Applications. Proceedings of 2011 IEEE AP-S International Symposium on Antennas and Propagation (IEEE AP-S 2011). Spokane, Washington, USA. 3–8 Jul 2011.

[32] Al-Husseini M, Safatly L, El-Hajj A, Kabalan K.Y, Christodoulou C.G (2012) Reconfigurable Filter Antennas for Pulse Adaptation in UWB Cognitive Radio Systems. Progress in electromagnetics research B. 37:327–342.

[33] Ebrahimi E, Hall P.S (2009) A Dual Port Wide-narrowband Antenna for Cognitive Radio. Proceedings of the third European Conference on Antennas and Propagation (EuCAP2009). Berlin, Germany. 23–27 Mar 2009. pp. 809–812

[34] Ebrahimi E, Kelly J.R, Hall P.S (2011) Integrated Wide-narrowband Antenna for Multi-standard Radio. IEEE transactions on antennas and propagation. 59:7:2628–2635.

[35] Al-Husseini M, Tawk Y, Christodoulou C.G, El-Hajj A, Kabalan K.Y (2010) A Reconfigurable Cognitive Radio Antenna Design. Proceedings of the 2010 IEEE AP-S International Symposium on Antennas and Propagation (IEEE AP-S 2010). Toronto, ON, Canada. 11–17 Jul 2010.

[36] Abu Tarboush H.F, Khan S, NilavalanR, Al-Raweshidy H.S, Budimir D (2009) Reconfigurable Wideband Patch Antenna for Cognitive Radio. Proceedings of the 2009 Loughborough antennas and propagation conference (LAPC 2009), Loughborough, UK. 16–17 Nov 2009. pp.141–144.

[37] Hamid M.R, Gardner P, Hall P.S, Ghanem F (2011) Switched-band Vivaldi Antenna. IEEE transactions on antennas and propagation. 59:5:1472–1480.

[38] Hamid M.R, Gardner P, Hall P.S, Ghanem F (2011) Vivaldi Antenna with Integrated Switchable Band Pass Resonator. IEEE transactions on antennas and propagation. 59:11:4008–4015.

[39] Al-Husseini M, Ramadan A, Zamudio M.E, Christodoulou C.G, El-Hajj A, Kabalan K.Y (2011) A UWB Antenna Combined with a Reconfigurable Bandpass Filter for Cognitive Radio Applications. Proceedings of the 2011 IEEE-APS Topical Conference on Antennas and Propagation in Wireless Communications (IEEE APWC 2011). Torino, Italy. 12–16 Sep 2011. pp. 902–904.

[40] Kazerooni M, Cheldavi A, Kamarei M (2009) A Novel Bandpass Defected Microstrip Structure (DMS) Filter for Planar Circuits. Proceedings of the 2009 Progress in Electromagnetics Research Symposium (PIERS 2009). Moscow, Russia. 18–21 Aug 2009. pp. 1214–1217.